ОБЪЕДИНЕННЫЙ
ИНСТИТУТ
ЯДЕРНЫХ
ИССЛЕДОВАНИЙ

Дубна

E4-98-179

Ş.Mişicu[1], D.Protopopescu[2]

DEFORMATION EFFECTS IN THE CLUSTER RADIOACTIVITY

Submitted to «Acta Physica Polonica B»

[1]Department of Theoretical Physics, National Institute for Nuclear Physics and Engineering, Bucharest-Mágurele, POB MG-6, Romania
[2]On leave of absence from: National Institute for Physics of Materials, Bucharest-Mágurele, POB MG-6, Romania

1998

I. INTRODUCTION

The theoretical study of the heavy-cluster emission and the super-asymmetric fission started at the end of seventies in Dubna by the romanian physicist A.Săndulescu and its collaborators [1]. Since the beginning this phenomenon was recognized to be a consequence of the shell closure of one or both fragments because of its cold nature, i.e. the low excitation energy involved in the process. Later on Rose and Jones confirmed experimentally the existence of this new phenomenon [2]. Since then many theoretical and experimental studies have been carried out (for a review see [3]). Recently it was advocated that the cluster radioactivity is not an isolated phenomenon, and must be related to other processes like the cold fusion or cold fission [4], where the closed shell effects play a dominant role. A still opened problem in the study of the cluster radioactivity is represented by the question of the existence of only the spherical or both the spherical and the deformed closed shells. Although both daughter and emitted cluster have in many cases, at least for even-even nuclei, a spherical shape in the ground state, according to the liquid drop model [5], nothing prevents us, in the cluster radioactivity process, to deal also with deformed shapes. Until now there are no experimental data available for deformed daughters. The first theoretical study of the cluster deformation effects on the WKB penetrabilities have been carried out by Săndulescu *et al.* [6] using the double folded Michigan-3 Yukawa (M3Y).

In this paper we extend the study of the deformation effects in cluster radioactivity by accounting also for the deformation of the daughter nucleus and including higher multipole deformations, like the hexadecupole one. The interaction between the daughter nucleus and the cluster, in the region of small overlap and throughout the barrier is computed by means of a double folding potential. The nuclear part includes a repulsive core at small distances. In this way our deformed cluster approach supposes a cluster already formed in the potential pocket coming from the interplay between the Coulomb and the repulsive nuclear core on one hand and the attractive nuclear force on the other hand. The depth and the wideness of this pocket will determine the assault frequency of the cluster on the barrier, through which it will eventually tunelate. In its turn, the penetrability will depend on the height and wideness of the barrier. Since all these geometrical characteristics depend sensitively on the shape of the fragments we will investigate in this paper the modification induced by the quadrupole and hexadecupole deformations of the fragments on the pocket and the barrier and finally compute decay rates for the disintegration reaction $^{224}\mathrm{Ra} \rightarrow {}^{210}\mathrm{Pb} + {}^{14}\mathrm{C}$.

II. CLUSTER-DAUGHTER DOUBLE-FOLDING POTENTIAL

The nuclear interaction between the daughter and the cluster can be calculated as the double folding integral of ground state one-body densities $\rho_{1(2)}(\boldsymbol{r})$ of heavy ions as follows

$$U_N(\boldsymbol{R}) = \int d\boldsymbol{r}_1 d\boldsymbol{r}_2 \; \rho_1(\boldsymbol{r}_1)\rho_2(\boldsymbol{r}_2)v(\boldsymbol{s}) \tag{1}$$

where v is the NN effective interaction and the separation distance between two interacting nucleons is denoted by $\boldsymbol{s} = \boldsymbol{r}_1 + \boldsymbol{R} - \boldsymbol{r}_2$ and R is the centre-to-centre distance. In the past a G-matrix M3Y effective interaction was used to discuss light and heavy cluster radioactivity. This interaction contains isoscalar and isovector Yukawa functions in each spin-isospin (S,T) channel and an exchange component coming from the one-nucleon knock-on exchange term. However, this interaction is based on density-independent nucleon-nucleon forces and consequently very deep nucleus-nucleus potentials are obtained. As have been shown by Adamian *et al.* [7], a double folding potential based on effective Skyrme interaction will contain a

repulsive core which would prevent, according to the Pauli principle, a large overlap of the two interacting nuclei.

Thus the interaction potential between two nuclei contains an attractive part and a repulsive part

$$U_N(\boldsymbol{R}) = C_0\left\{\frac{F_{in}-F_{ex}}{\rho_{00}}\Big((\rho_1^2 * \rho_2)(\boldsymbol{R}) + (\rho_1 * \rho_2^2)(\boldsymbol{R})\Big) + F_{ex}(\rho_1 * \rho_2)(\boldsymbol{R})\right\} \tag{2}$$

where $*$ denotes the convolution of two functions f and g, i.e. $(f * g)(\boldsymbol{x}) = \int f(\boldsymbol{x}')g(\boldsymbol{x}-\boldsymbol{x}')d\boldsymbol{x}'$. The values of the constants $C_0, F_{in}, F_{ex}, \rho_{00}$ are given in ref. [7]. To solve this integral we consider the inverse Fourier transform

$$U_N(\boldsymbol{R}) = \int e^{-i\boldsymbol{q}\cdot\boldsymbol{R}}\tilde{U}_N(\boldsymbol{q})d\boldsymbol{q} \tag{3}$$

where the Fourier transform of the local Skyrme potential $\tilde{U}_N(\boldsymbol{q})$ can be casted in the form

$$\tilde{U}_N(\boldsymbol{q}) = C_0\left\{\frac{F_{in}-F_{ex}}{\rho_{00}}\Big(\widetilde{\rho_1^2}(\boldsymbol{q})\tilde{\rho}_2(-\boldsymbol{q}) + \tilde{\rho}_1(\boldsymbol{q})\widetilde{\rho_2^2}(-\boldsymbol{q})\Big) + F_{ex}\tilde{\rho}_1(\boldsymbol{q})\tilde{\rho}_2(\boldsymbol{q})\right\} \tag{4}$$

where $\tilde{\rho}(\boldsymbol{q})$ and $\widetilde{\rho^2}(\boldsymbol{q})$ are Fourier transforms of the nucleon densities $\rho(\boldsymbol{r})$ and squared nuclear densities $\rho(\boldsymbol{r})^2$. Expanding the nucleon densities for axial-symmetric distributions in spherical harmonics, we get

$$\rho(\boldsymbol{r}) = \sum_\lambda \rho(r)Y_{\lambda 0}(\theta,0) \tag{5}$$

Then

$$\tilde{\rho}(\boldsymbol{q}) = 4\pi\sum_\lambda i^\lambda Y_{\lambda 0}(\theta_q,0)\int_0^\infty r^2 dr \rho_\lambda(r)j_\lambda(qr) \tag{6}$$

$$\widetilde{\rho^2}(\boldsymbol{q}) = 4\pi\sum_\lambda i^\lambda Y_{\lambda 0}(\theta_q,0)\frac{\hat{\lambda}'\hat{\lambda}''}{\sqrt{4\pi}\hat{\lambda}}(C^{\lambda\lambda'\lambda''}_{0\,0\,0})^2\int_0^\infty r^2 dr \rho_{\lambda'}(r)\rho_{\lambda''}(r)j_\lambda(qr) \tag{7}$$

In this paper we take the one-body densities for both daughter and cluster as two-parameter Fermi distributions in the intrinsic frame for axial symmetric nuclei

$$\rho(r) = \frac{\rho_{00}}{1+\exp((r-R(\theta))/a)} \tag{8}$$

Here $\rho_{00} = 0.17$ fm, a denotes the diffusivity which is taken to be 0.63 for the daughter and 0.67 for the cluster, and

$$R(\theta) = R_0 \left(1 + \beta_2 \sqrt{\frac{5}{4\pi}} P_2(\cos\theta) + \beta_4 \frac{3}{\sqrt{4\pi}} P_4(\cos\theta)\right) \tag{9}$$

is the parameterization of the nuclear shape in quadrupole β_2 and hexadecupole β_4 deformations. Here $R_0 = r_0 A^{1/3}$ with r_0 computed by means of a liquid drop prescription [5].

III. CALCULUS OF DECAY CONSTANTS

We adopt a modified Gammow approach [3] which is based on the idea that the cluster is pre-born, with a certain probability P_0, in the pocket of the Migdal+Coulomb potential and later on it tunnels through an essentially one-dimensional barrier. Consequently the decay rate λ will be defined as follows:

$$\lambda = \nu_0 P_0 P \tag{10}$$

where ν_0 is the assault frequency with which the cluster bombards the walls of the potential pocket. It is given by the inverse of the classical period of motion

$$T_0 = \int_{r_{t1}}^{r_{t2}} dr \sqrt{\frac{2\mu}{Q-V(r)}} \tag{11}$$

where μ is the reduced mass of the cluster-daughter pair and r_{t1} and r_{t2} are the inner turning points, where the potential curve intersects the Q-value (see Fig.1). Thus, in our model, ν_0 depends sensitively on the size of the potential pocket. The barrier penetrability is given by the well known WKB formula

$$P = \exp\left(-2\int_{r_{t2}}^{r_{t3}} dr \sqrt{\frac{2\mu}{\hbar^2}(U(r)-Q)}\right) \tag{12}$$

where r_{t3} is the outer turning point.

The calculus of the preformation probability P_0 is usually based on elaborated microscopic models. Since its calculation is beyond the purpose of this material, we limit ourselves to a simple empirical formula proposed by Blendowske *et.al.* [8] for α, ^{12}C, ^{14}C and ^{16}O clusters

$$P_0 = (P_0^\alpha)^{\frac{A_c-1}{3}} \qquad A_c \leq 28 \tag{13}$$

where the subscript c refers to the cluster and the α-spectroscopic factor is estimated as

$$(P_0^\alpha)^{even} = 6.3\times10^{-3} \quad \text{and} \quad (P_0^\alpha)^{odd} = 3.2\times10^{-3} \tag{14}$$

In what follows we consider the ^{14}C-decay of ^{224}Ra.

In figure Fig.1 we plotted a family of potential curves $U(R)$ for several quadrupole deformation β_2^C of the cluster ^{14}C and fixed hexadecupole deformation of the daughter β_4^D which is chosen to be 0.008, i.e. the ground state value for ^{210}Pb. As one can see on this plot, the increase of β_2^C from negative to positive values is accompanied by the lowering of the barrier, while the bottom of the pocket goes down further. The decay rate is influenced by the changes with deformation in the region between the first turning point and the top of the barrier. The figures show only this part of the potential curve.

For comparison, the next plot, Fig.2, shows the variation of the interaction potential with the hexadecupole deformation of the cluster. The variation brought by the hexadecupole deformation is slightly different. Here the barrier lowers also with β_4^C, but the bottom of the pocket rises. One might expect that this will affect the values of life-times in a different way than the one β_2^C does.

Plots of the interaction potential $U(R)$ for different pairs $(\beta_2^D;\beta_2^C)$ of quadrupole deformation are shown in Fig.3. One can compare the magnitude of the effect of both cluster and daughter quadrupole deformations and the changes which occur when we pass from prolate to oblate deformation. One can notice that the quadrupole deformation β_2^C of the cluster acts mainly on the right wall of the pocket, while the modification of the quadrupole deformation of the daughter nucleus push in opposite directions both walls of the pocket.

The difference between positive and negative quadrupole and hexadecupole deformations of the daughter nucleus can be easily understood from Fig.4. We observe different type of modifications in the shape of the pocket, corresponding to β_2 and β_4 deformations, respectively. The quadrupole and hexadecupole deformations of the daughter change the depth of the potential pocket in the same manner, in comparison with the case of cluster deformations which, as we saw in Fig.2, move the bottom of the pocket in opposite directions.

A plot of calculated λ, as function of the deformations of the daughter nucleus is drawn in Fig.5. In our calculations, the λ-s close to the experimental value, correspond to deformed configurations. One might notice that the effects of the quadrupole and hexadecupole deformations are almost of the same magnitude.

The same is done in the next figure but for cluster deformations (see Fig.6). Here we compare the dependencies of the decay constant on β_2^C and β_4^C. The difference in slope between the two curves is much evident than in the precedent figure. This fact is easily understood by recalling the observations made earlier (see figures 1 and 2), on the modification of the barrier due to the quadrupole and hexadecupole deformations. The hexadecupole deformation of the cluster increases the pocket depth (see Fig.1) and consequently ν_0 will increase too, while the increase of hexadecupole deformation of the cluster is accompanied by the rise of the bottom of the potential pocket and the lowering of the barrier height is partly compensated by the diminution of ν_0.

In table I we selected some of the most favorable cases for our calculated decay

rates. From here we infer the importance of daughter's deformation. The value corresponding to case 1 is obtained when considering both nuclei in their ground state deformations. As we expected, prolate deformations (see cases 7, 11-18) favor the decay. Deformations around 0.04 either in β_2 or in β_4 of the daughter nucleus give us decay rates close to the experimental one. One can notice that acceptable values of λ are reached more convenient through deformations of the daughter nucleus, than through deformations of the cluster (see cases 15-18). Case 5 shows that even an oblate shape for the emitted cluster can be taken into discussion. If we remind that the mother nucleus ^{224}Ra has a prolate deformed ground state $\beta_2 = 0.17$, one might suppose that such a picture - prolate daughter and an oblate cluster - is intuitively acceptable.

IV. CONCLUSIONS

The aim of this paper was to extend previous studies of deformation effects in cluster radioactivity by considering also the deformation of the daughter nucleus and to include the next higher even deformation, the hexadecupole one. Considering that the cluster is pre-born in the potential pocket produced by the interplay between repulsive and attractive forces we investigated the modifications induced by deformations on the specific potential that we employ. The computed decay rates depends on the assault frequency, which varies with the pocket depth, and on the penetrability, which changes with the barrier height. We showed that the experimental values can be reproduced for several selections of the deformations. If we maintain the cluster spherical and vary the quadrupole and/or hexadecupole deformations of the daughter nucleus we may reach the experimental value within a reasonable range of deformations parameters. Another interesting result is that even for an oblate deformation of the cluster we may obtain decay rates close to the experimental value.

Case	Cluster		Daughter		λ
$\mathcal{N}^o$	β_2	β_4	β_2	β_4	$(10^{-17}s^{-1})$
1	0.000	0.000	0.000	0.008	0.67
2			-0.020	0.008	0.10
3	0.050		-0.020	0.008	0.33
4			0.025	0.008	4.12
5	-0.050		0.050	0.008	8.62
6			0.050	0.008	18.52
7			0.020	-0.012	0.49
8			0.020	0.006	2.51
9		0.025		0.008	0.75
10	0.025			0.008	1.11
11	0.050			0.008	1.73
12			0.040		5.90
13				0.040	9.47
14			0.020	0.023	9.04
15	0.080			0.008	3.01
16	0.130			0.008	7.23
17		0.100		0.008	1.16
18	0.100	0.050		0.008	5.76

Table I. Comparison between the calculated decay constants λ corresponding to different deformations. For the case in discussion, ^{224}Ra $\rightarrow$ ^{210}Pb$+^{14}$C, the experimental value of the decay constant is $\lambda_{exp} = 9.50 \times 10^{-17}$ s^{-1}. Empty spaces in the table mean null values.

FIGURES

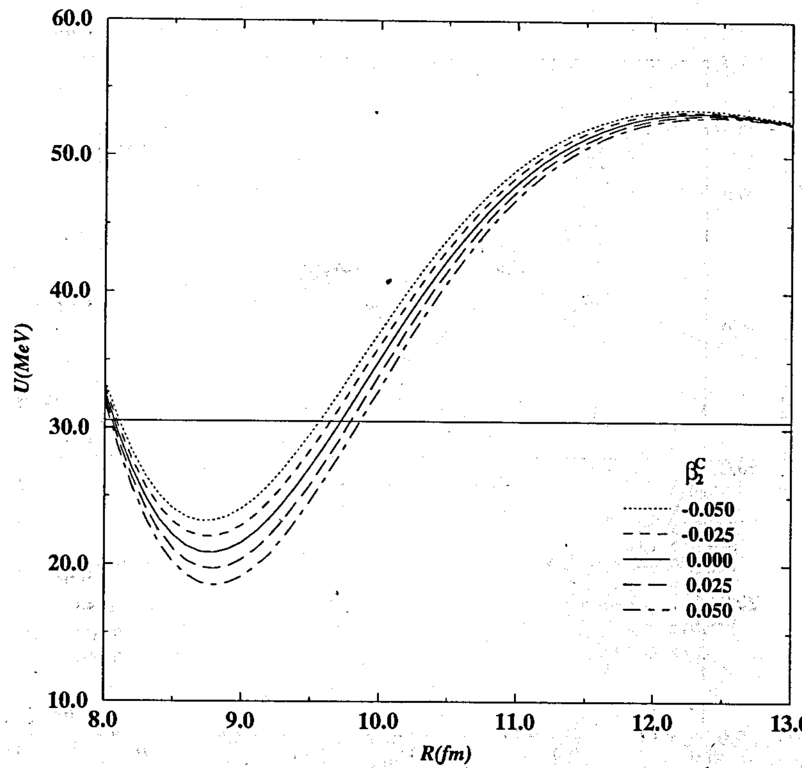

Figure 1. Variation of the interaction potential $U(R)$ with the quadrupole deformation of the cluster, β_2^C, when the ground hexadecupole deformation for ^{210}Pb is kept fixed, i.e. $\beta_4^D = 0.008$. The distance R is measured between the centers of mass of the two nuclei. The horizontal line at 30.53 MeV is the Q-value of the decay.

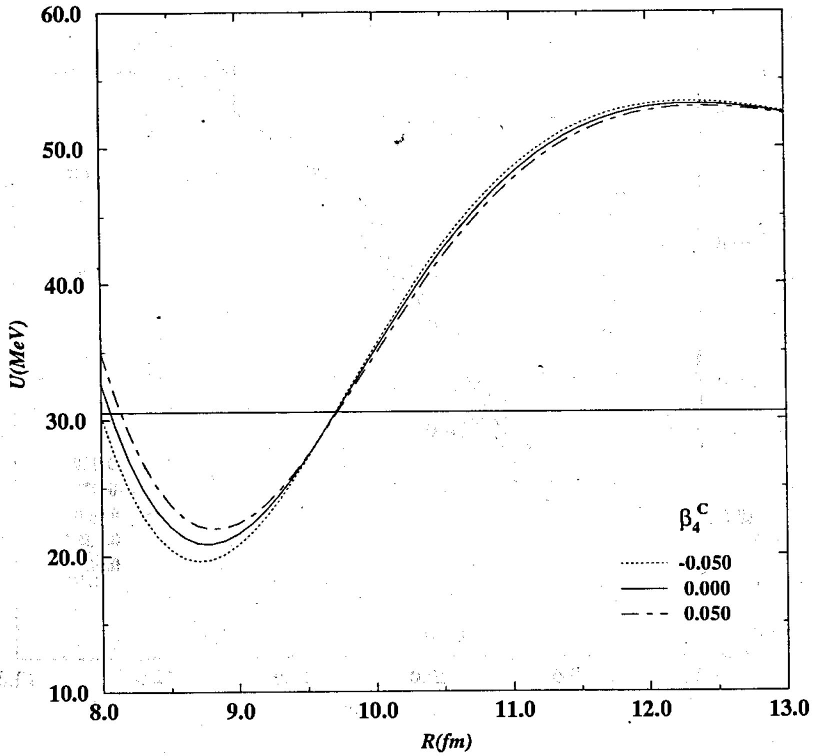

Figure 2. Variation of the interaction potential $U(R)$ with the hexadecupole deformation of the cluster, β_4^C. All deformation parameters, except β_4^D=0.008, are zero.

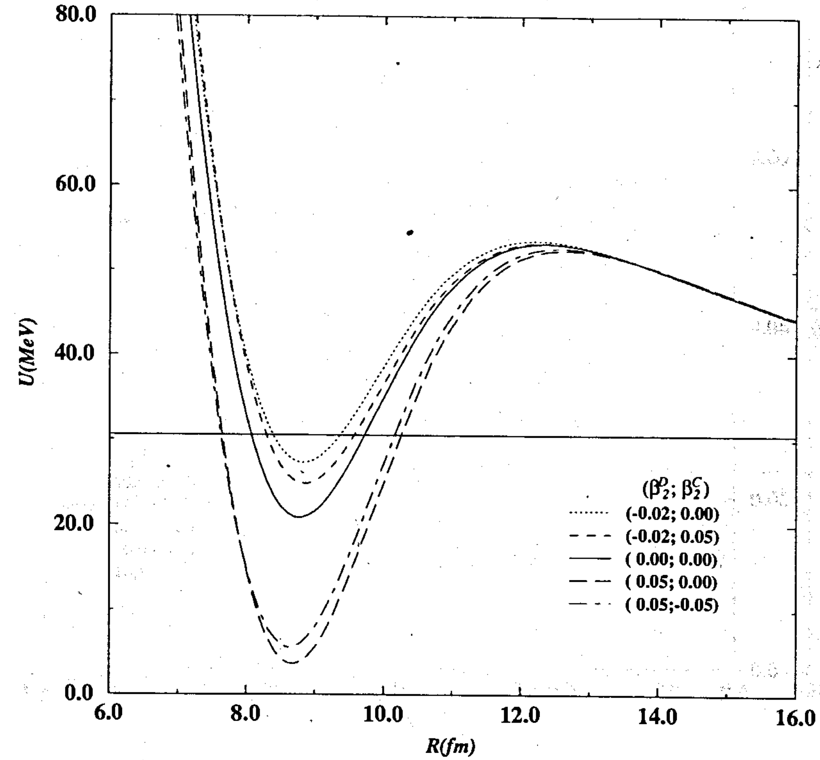

Figure 3. Plots of the interaction potential $U(R)$ for different pairs of daughter-cluster quadrupole deformation (β_2^D;β_2^C).

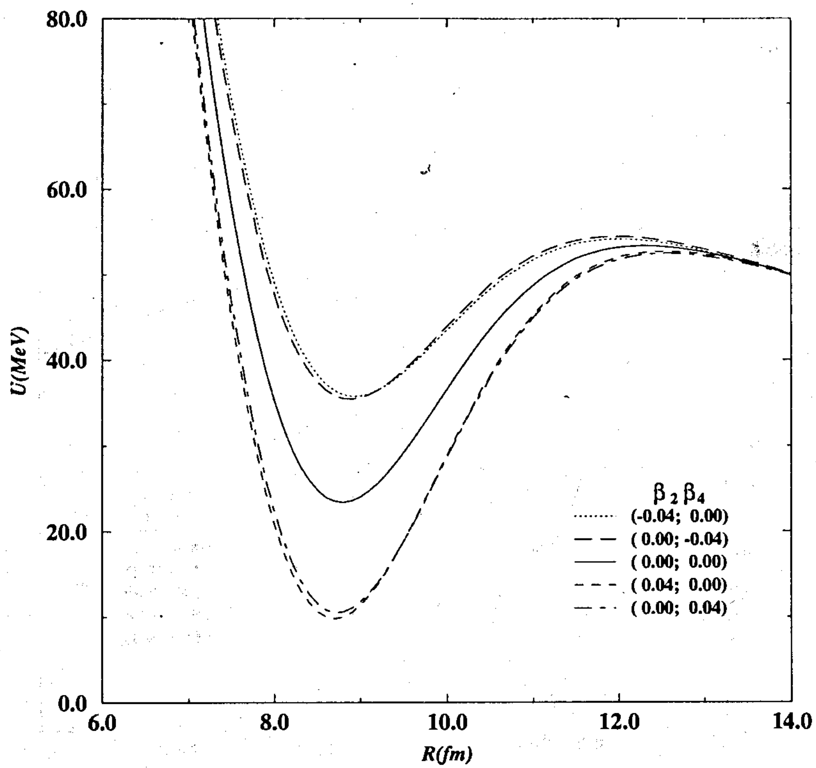

Figure 4. Comparison between the effects of quadrupole and hexadecupole deformations of the daughter nuclei. Here, contrary to the case when the cluster is deformed, the quadrupole and hexadecupole deformations modify the depth of the pocket in the same manner.

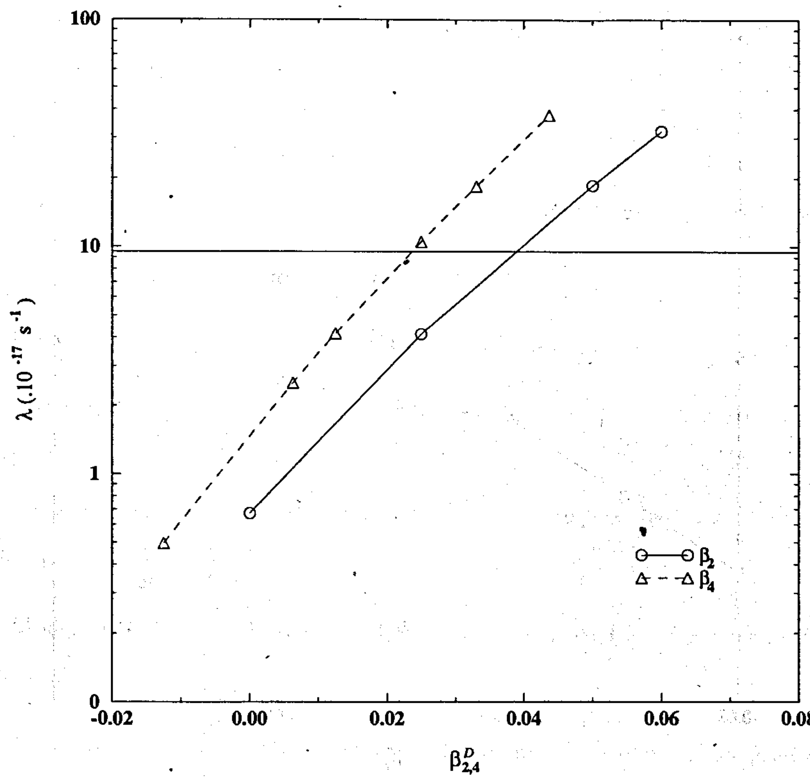

Figure 5. Plots of the decay rate versus β_2^D (solid line) and β_4^D (dashed line). The hexadecupole dependency is drawn with β_2^D =0.02. The cluster is spherical in both cases. The full horizontal line represents the experimental value for the discussed decay, $\lambda_{exp} = 9.50 \times 10^{-17}$ s^{-1}.

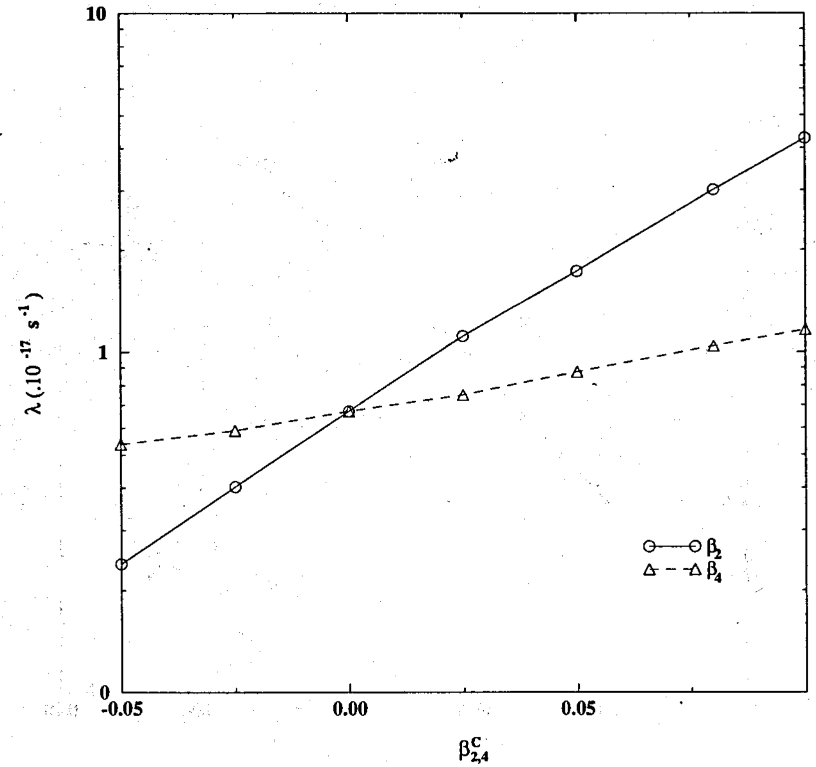

Figure 6. The dependency of the decay constant λ on β_2^C (solid line) and β_4^C (dashed line). A deformed state of the daughter is needed in order to reach the experimental λ within reasonable values of cluster deformation. The daughter nucleus is taken in its ground state deformation.

In conclusion the study carried out in this paper points mainly to the importance of the daughter nucleus deformations, and especially its hexadecupole one.

REFERENCES

[1] A.Săndulescu, D.N.Poenaru and W.Greiner, *Sov.J.Part.Nucl.* **11**, 528 (1980).

[2] H.J.Rose and G.A.Jones, *Nature* **307**, 245 (1984).

[3] R.K.Gupta and W.Greiner, *Int.J.Mod.Phys.* **3**, 335 (1994).

[4] A. Săndulescu, A. Florescu and W. Greiner, *J. Phys. G: Nucl. Part.Phys.* **15**, 1815 (1989).
S.Singh, R.K.Gupta, W.Scheid and W.Greiner, *J.Phys. G: Nucl.Part.Phys.* **18** , 1243 (1992).

[5] P. Möller, J.R. Nix, W.D. Myers and W.J. Swiatecki, *At.Data Nucl. Data Tables* **59**, 185 (1995).

[6] A.Săndulescu, R.K.Gupta, F.Cârstoiu, M.Horoi and W.Greiner, *Int.J.Mod.Phys.* **E1**, 379 (1992).
R.K.Gupta, M.Horoi, A.Săndulescu, M.Greiner and W.Scheid, *J.Phys. G: Nucl.Part.Phys.* **19**, 2063 (1993)

[7] G.G.Adamian, N.V.Antonenko, R.V.Jolos, S.P.Ivânova and O.I.Melnikova, *Int.J.Mod.Phys. E* **5**, 191 (1996).

[8] R.Blendowske, T.Fliessbach and H.Walisser, *Z.Phys.* **A339**, 191 (1991).

Received by Publishing Department
on June 22, 1998.